Synthesis of $^{197m/g}$Hg labelled gold nanoparticles for targeted radionuclide therapy

Droop, Philipp; Chen, Shaohuang; Radford, Melissa J.; Paulssen, Elisabeth; Gates, Byron D.; Reilly, Raymond M.; Radchenko, Valery; Hoehr, Cornelia

DOI
10.1515/ract-2023-0144

Publication date
2023

Document Version
Final published version

Published in
Radiochimica Acta

Philipp Droop, Shaohuang Chen, Melissa J. Radford, Elisabeth Paulssen, Byron D. Gates, Raymond M. Reilly, Valery Radchenko and Cornelia Hoehr*

Synthesis of $^{197m/g}$Hg labelled gold nanoparticles for targeted radionuclide therapy

https://doi.org/10.1515/ract-2023-0144
Received February 6, 2023; accepted July 15, 2023;
published online July 28, 2023

Abstract: Meitner-Auger-electron emitters have a promising potential for targeted radionuclide therapy of cancer because of their short range and the high linear energy transfer of Meitner-Auger-electrons (MAE). One promising MAE candidate is $^{197m/g}$Hg with its half-life of 23.8 h and 64.1 h, respectively, and high MAE yield. Gold nanoparticles (AuNPs) that are labelled with $^{197m/g}$Hg could be a helpful tool for radiation treatment of glioblastoma multiforme when infused into the surgical cavity after resection to prevent recurrence. To produce such AuNPs, $^{197m/g}$Hg was embedded into pristine AuNPs. Two different syntheses were tested starting from irradiated gold containing trace amounts of $^{197m/g}$Hg. When sodium citrate was used as reducing agent, no $^{197m/g}$Hg labelled AuNPs were formed, but with tannic acid, $^{197m/g}$Hg labeled AuNPs were produced. The method was optimized by neutralizing the pH (pH = 7) of the Au/$^{197m/g}$Hg solution, which led to labelled AuNPs with a size of 12.3 ± 2.0 nm as measured by transmission electron microscopy. The labelled AuNPs had a concentration of 50 µg (gold)/mL with an activity of 151 ± 93 kBq/mL (^{197g}Hg, time corrected to the end of bombardment).

***Corresponding author: Cornelia Hoehr**, Life Sciences Division, TRIUMF, Vancouver, BC V6T 2A3, 4004 Wesbrook Mall, Canada,
E-mail: choehr@triumf.ca
Philipp Droop, Life Sciences Division, TRIUMF, Vancouver, BC V6T 2A3, 4004 Wesbrook Mall, Canada; and Faculty of Chemistry and Biotechnology, FH Aachen, 52428 Jülich, Heinrich-Mußmann-Straße 1, Germany
Shaohuang Chen, Life Sciences Division, TRIUMF, Vancouver, BC V6T 2A3, 4004 Wesbrook Mall, Canada; and Department of Chemistry, Simon Fraser University, Burnaby, BC V5A 1S6, 8888 University Dr, Canada
Melissa J. Radford and Byron D. Gates, Department of Chemistry, Simon Fraser University, Burnaby, BC V5A 1S6, 8888 University Dr, Canada
Elisabeth Paulssen, Faculty of Chemistry and Biotechnology, FH Aachen, 52428 Jülich, Heinrich-Mußmann-Straße 1, Germany; and Department of Radiation Science and Technology, TU Delft, 2698 JB Delft, Mekelweg 15, Delft, The Netherlands
Raymond M. Reilly, Leslie Dan Faculty of Pharmacy, University of Toronto, Toronto, ON M5S 1A1, 144 College St, Canada
Valery Radchenko, Life Sciences Division, TRIUMF, Vancouver, BC V6T 2A3, 4004 Wesbrook Mall, Canada; and Department of Chemistry, University of British Columbia, Vancouver, V6T 1Z4, Canada

Keywords: $^{197m/g}$Hg; gold nanoparticle (AuNP); Meitner-Auger-electron (MAE); targeted radionuclide therapy (TRT)

1 Introduction

Due to their short range and high Linear Energy Transfer (LET), Meitner-Auger-electrons (MAE) are a promising candidate for targeted radionuclide therapy (TRT). High doses can be delivered to a small tissue volume sparing the surrounding healthy tissue [1]. One promising candidate for TRT with MAE is $^{197m/g}$Hg. Both isomers can be produced simultaneously by bombarding natural gold (100 % Au-197) with protons, with maximum cross sections at 10 MeV (^{197g}Hg) and 12 MeV (^{197m}Hg), respectively, making production at a medical cyclotron possible [2]. Figure 1 illustrates the decay of $^{197g/m}$Hg. ^{197m}Hg decays to ^{197g}Hg via internal conversion (IC) or via electron capture (EC) to 197Au [3]. In this process, on average 19.4 MAE are emitted per decay with an average total energy of 7.6 keV [4]. ^{197g}Hg decays via electron capture to 197Au [3]. In this process, on average 23.2 MAE are emitted with an average total energy of 7.4 keV [4]. It should be noted that the internal transitions are highly converted and so the intensities of gamma rays given are weak.

All these characteristics of $^{197m/g}$Hg make it suitable for TRT of cancers like glioblastoma multiforme (GBM), which is one of the most common and deadliest brain cancers [5]. Due to its high infiltration of the brain on a cellular level and efficient self-renewing abilities [6], patients diagnosed with GBM have a mean survival of only 11.6 ± 12.1 months [7]. One possible tool to combat recurrence and to prolong the survival of patients could be the infusion of $^{197m/g}$Hg labelled gold nanoparticles (AuNPs) into the surgical cavity after tumor resection. Efforts employing AuNP labelled with ^{177}Lu show promising results [8].

AuNPs are already used in radiotherapy as radiosensitizers, because of their biocompatibility, size range, absorption of X-rays, and coating options [9–11]. Their distribution *in vivo* is dependent on their size and shape range. To synthesize monodisperse gold nanoparticles, a variety of synthetic methods are well established. Spherical AuNPs can be produced by reduction of gold ions. Size and shape of the resulting nanoparticles are dependent on the solution

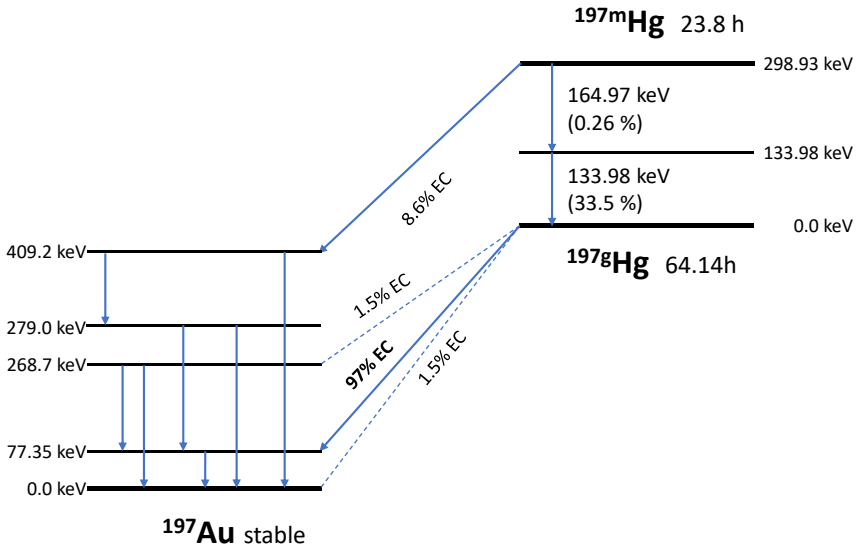

Figure 1: Decay chart of $^{197m/g}$Hg. Data from [3].

composition and concentrations of the initial reagents, choice of reducing agent, and pH [12].

Our goal was to produce $^{197m/g}$Hg labelled AuNPs, which could be used for TRT. The average energy of the Auger electrons are 7.4 keV and 7.6 keV for ^{197g}Hg and ^{197m}Hg, respectively [13]. Estimating their range in gold via the stopping power [14] results in a range of around 275 nm. It is therefore important to create the AuNP as small as possible to preserve the energy of the Auger electrons for the therapeutic application. One possible production route to such labelled AuNPs is the irradiation of AuNPs with protons in a liquid-target setup, i.e. the irradiation of a suspension of AuNPs. In previous work by our group, only low activities of 10.2 ± 0.4 kBq (^{197g}Hg) and 10.4 ± 0.9 kBq (^{197m}Hg) decay corrected to end of bombardment (EOB) were produced. During the irradiation, the AuNPs clustered together and resulted in a change in their size and shape [13] and the development of a liquid-target approach was not pursued further.

Alternatively, as described here the AuNPs were labeled with the $^{197m/g}$Hg already present prior to their synthesis. A solid gold target was irradiated, dissolved, and then AuNPs were formed from the solution containing the trace amount of $^{197m/g}$Hg created during the bombardment of the initial gold target.

2 Materials and methods

2.1 Chemicals and consumables

All chemicals, including sodium citrate, sodium carbonate, tannic acid, concentrated hydrochloric acid and concentrated nitric acid were purchased from Sigma-Aldrich (Canada) and used without further purification. Consumables like Falcon tubes (15 and 50 mL), 1.5 mL Eppendorf caps, 3 mL syringes, nonbleeding pH paper (pH 4 to 10), and syringe membrane filters of 0.45 µm, 0.2 µm and 0.02 µm were also supplied by Sigma Aldrich. Water was used from a Milli-Q dispenser with a conductivity of 18.2 MΩ cm. at 25 °C The gold for the irradiation was obtained from TRIUMF's internal inventory of legacy supply.

2.2 Au irradiation

A solid gold target (thickness: about 0.13 mm) on a tantalum backing (diameter: 28 mm, thickness: 1.0 mm) with an indent was manufactured. For this purpose, the tantalum backing was prepared by grinding the surface with sandpaper, heating with ammonium hexafluorosilicate, and scratching with tweezers to increase the surface area for better adhesion and to remove the surface oxidation layer. Around 250 mg of flattened gold was then placed into the recess in the backing. At a temperature of 1150 °C the gold was melted onto the backing. The target was subsequently mounted onto a 13 MeV cyclotron at TRIUMF in a dedicated solid target holder [15]. Irradiation with protons took place at a current of 20 µA and an energy of 12.8 MeV on the target surface for 4 h.

2.3 Production of the AuNPs

After irradiation, target removal and transport to the radiochemistry laboratory, the irradiated target was dissolved in few drops of aqua regia. The solution was evaporated close to dryness. Concentrated HCl was added and evaporated to remove the remaining nitric acid from the aqua regia. (*Caution*: *these acids are corrosive and should be handled with care*.) This step was repeated three times and the resulting tetrachloroauric (III) acid was dissolved in 37 mL water [16]. From this solution, a small aliquot was taken (about 5 % of the combined activity of $^{197m/g}$Hg) and AuNPs were produced using two different published methods. Both of these methods were first tested with non-irradiated Au targets, as well as by spiking Au with non-radioactive, natural Hg:

(A) In the method reported by Turkevich [17] 300 µL tetrachloroauric (III) acid (1 % w/w) was diluted in 30 mL boiling water, and 600 µL

sodium citrate (1 % w/w) was added. After boiling for 10 min, the suspension was cooled to room temperature.

(B1) In the method by Hatschek [18] 400 µL tetrachloroauric (III) acid (1 % w/w) was dissolved in 45 mL water, and 2.5 mL of fresh tannic acid solution (0.1 % w/w) was added in 0.5 mL increments while continuously stirring the solution.

(B2) In a small deviation from method (B1), the acid solution was neutralized with 10–15 drops of sodium carbonate (20 g/L) until reaching pH = 7, before 2.5 mL of fresh tannic acid solution (0.1 % w/w) was added in 0.5 mL steps while stirring this mixture.

2.4 Characterization of the AuNPs

Centrifugation was used to separate AuNPs from the liquid solution with a Sorvall Legend Micro 21R Centrifuge by Thermo Scientific for 1.5 mL tubes (REF:75,002,446).

The purity of the Au in the AuNPs was measured via an Inductively Coupled Plasma Mass Spectrometer (ICP-MS) from Agilent Technologies (Model No.:G3665A #100). The calibration was performed with a solution of HgCl2.

The size and shape of the AuNPs was determined using a Transmission Electron Microscope (TEM) (FEI Tecnai Osiris STEM). Samples were prepared for TEM analysis by drop-casting 5 µL of AuNP solution onto individual TEM grids (Formvar/Carbon Supported Copper Grids size 300 mesh, TEM-FCF300Cu from Sigma Aldrich). The grids were dried overnight in a vacuum desiccator prior to analysis. After confirming the shape of the AuNPs with the TEM, Dynamic Light Scattering (DLS) was used to estimate the size of the spherical AuNPs (Zetasizer Ultra Red Label, ZSU3305 from Malvern Pananalytical). The Zetasizer Ultra Red Label DLS had a 10 mW He–Ne 632.8 nm laser. Samples were diluted for DLS analysis with 18.2 MΩ-cm at 25 °C deionized water, then vortexed for 30 s. Next, 1.0 mL of sample was transferred into individual plastic semi-micro cuvettes (759,150 from BrandTech Scientific, Inc.) and capped, then immediately analyzed. The DLS measurements were collected using a non-invasive back-scattering mode with a detection angle of 173° and at a constant temperature of 25 °C for all samples. Triplicate measurements were performed for each sample.

For a convenient size estimate of the radioactive AuNPs, the solution was filtered through different size membrane filters with pore sizes of 0.45 µm, 0.2 µm and 0.02 µm.

All radioactivity measurements were performed with a high purity germanium (HPGe) radiation detector by Canberra (Model No.: 747), calibrated to a 20 mL ^{152}Eu source. Samples were assayed around 70 h after bombardment with a dead time of less than 3 %.

3 Results and discussion

3.1 AuNP production using method (A)

Method (A) was first tested with non-irradiated Au targets. The amount of natural Hg added to the solution before AuNP formation was 24 ppb. The resulting brown-red solution was centrifuged, and the overlaying solution (supernatant) without the AuNPs was measured via ICP-MS. After the AuNP formation, the amount of Hg measured in the solution was 2.9 ppb, suggesting that Hg was embedded in the AuNPs.

When tested using the radioactive solution of gold containing $^{197m/g}$Hg, it was not possible to produce any AuNPs using method (A). Even with doubling the amounts of the sodium citrate reducing agent no stable nanoparticles could be produced. One reason could be the presence of nitric acid in the gold solution, remaining in small amounts from the dissolution process. The presence of nitric acid prevents or reverses the reduction of gold. During the evaporation step, the solution is typically heated to complete dryness. But to avoid radioactive contamination to our fume hood, in method (A) the radioactive solution was only heated to just before dryness, leaving small amounts of nitric acid in the resulting gold solution as indicated by the pH value of the solutions. The non-radioactive gold solution had a pH of 4 after evaporation, while the radioactive solution had a pH of 2. Method (A) was abandoned in this work as no radioactive AuNPs were achieved.

3.2 AuNP production with method (B)

Method (B1) produced non-radioactive AuNPs as well. The amount of natural Hg added to the solution before AuNP formation was 16 ppb. After AuNP formation that resulted in a violet-red solution color, the amount of Hg measured in the solution without the AuNPs (i.e. supernatant resulting from isolating the particles by centrifugation) was under the detection limit, again suggesting that the Hg was embedded into the AuNP.

With method (B1) it was possible to produce radioactive AuNPs, with Hg embedded into the nanoparticles. The produced AuNPs were centrifuged, and the supernatant was collected. The resulting AuNPs were rinsed with deionized water and separated again by centrifugation. The radioactivity in the three fractions collected (i.e. AuNP as solids, initial supernatant, and wash solution) were each measured via HPGe, see Figure 2. It is clear from the figure that the majority of the radioactivity is embedded or at least firmly attached in the AuNPs. Embedding of the radionuclide in the nanoparticle matrix is important to prevent the $^{197m/g}$Hg from detaching from the AuNPs in the proposed *in-vivo* application.

To assess the size of the nanoparticles shortly after irradiation, the AuNPs were filtered with membrane filters and the resulting solutions were measured with HPGe, see Figure 3. Over 60 % of the radioactivity was captured within the AuNPs that had a size greater than 200 nm but smaller than 450 nm. As this variation in size is rather large, the reaction conditions were adjusted to produce smaller

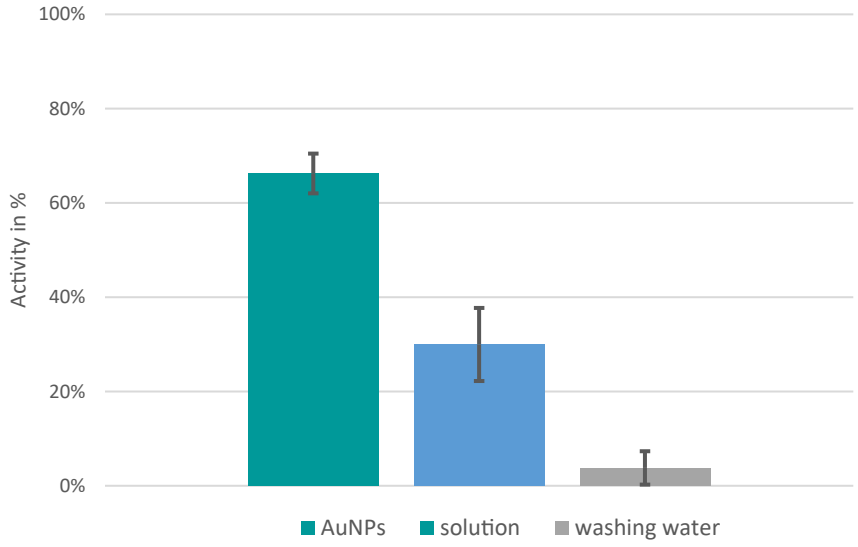

Figure 2: Percentage of total radioactivity of $^{197m/g}$Hg in the AuNPs [Method (B1)], in the supernatant solution, and in the water used to rinse the AuNPs.

nanoparticles. The diluted tetrachloroauric (III) acid was neutralized before the production of the AuNPs [method (B2)]. The resulting size distribution is shown in Figure 4. The AuNPs smaller than 20 nm contained (96 ± 7) % of the activity, indicating that most of the AuNPs were smaller than 20 nm. The total activity of the AuNPs in the diluted solution was (151 ± 93) kBq/mL (solution), decay-corrected to end-of-bombardment (EOB). This is averaged over three different productions. The highest amount achieved in a single production, decay-corrected to EOB, was (4.7 ± 0.5) MBq/mg (gold) for ^{197g}Hg, and (55.6 ± 1.2) MBq/mg (gold) for ^{197m}Hg.

To obtain a more detailed view of the size and shape of the AuNPs, they were analyzed by TEM, such as the image in Figure 5, corresponding to non-radioactive AuNPs without the addition of Hg. These nanoparticles have a spherical shape and an average diameter of 12.2 ± 3.2 nm determined by measuring 118 nanoparticles, see Figure 5 for the corresponding histogram for the size distribution.

To investigate the impact of mercury inside the AuNPs on their shape and size, AuNPs spiked with 16 ppb non-radioactive mercury were also imaged, see Figure 6. Several spherical AuNPs are visible with an average size of 10.5 ± 2.2 nm determined by measuring 253 different nanoparticles. This demonstrates that the addition of Hg to the solution before the formation of AuNPs does not change the shape or significantly affect the overall size of the nanoparticles.

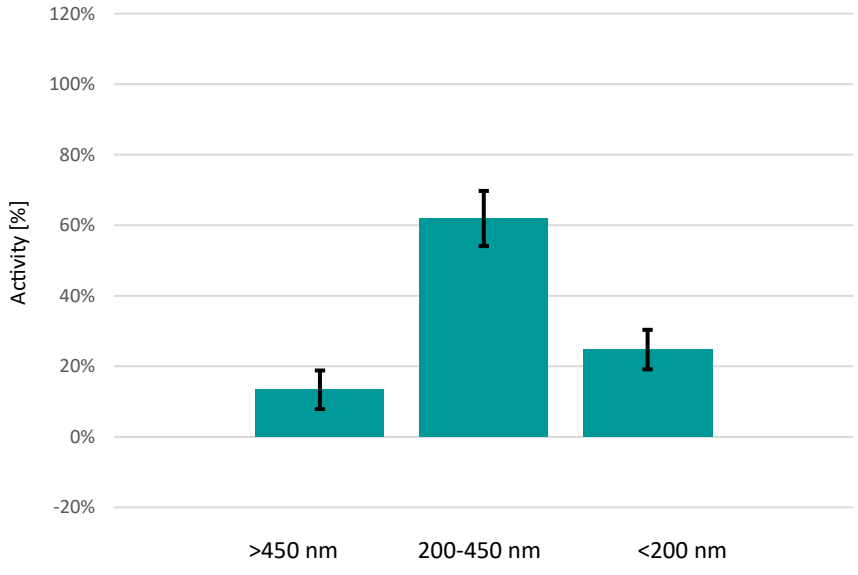

Figure 3: Percentage of total radioactivity of $^{197m/g}$Hg in the AuNP as a function of size [Method (B1)].

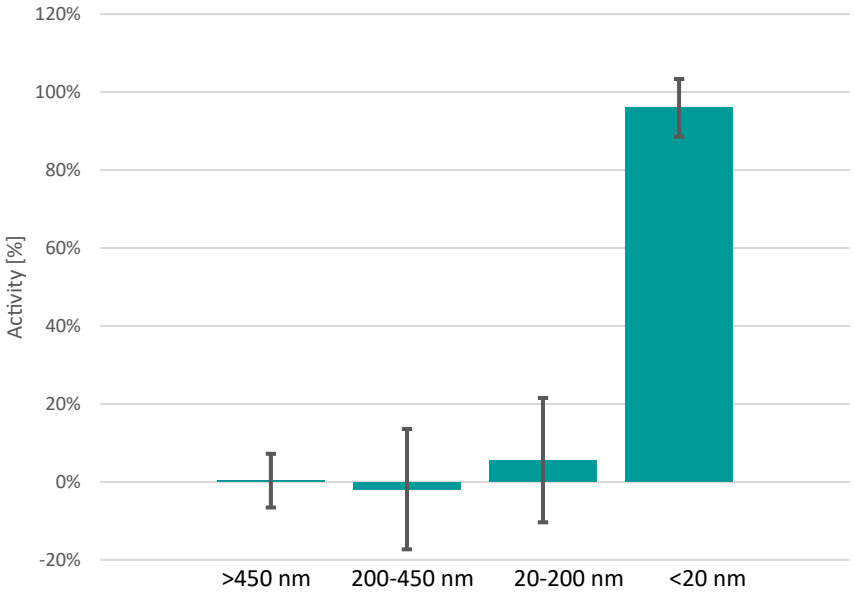

Figure 4: Percentage of the total activity of $^{197m/g}$Hg found in the AuNPs [Method (B2)] collected in the fractions of the solution after filtration through specific filters.

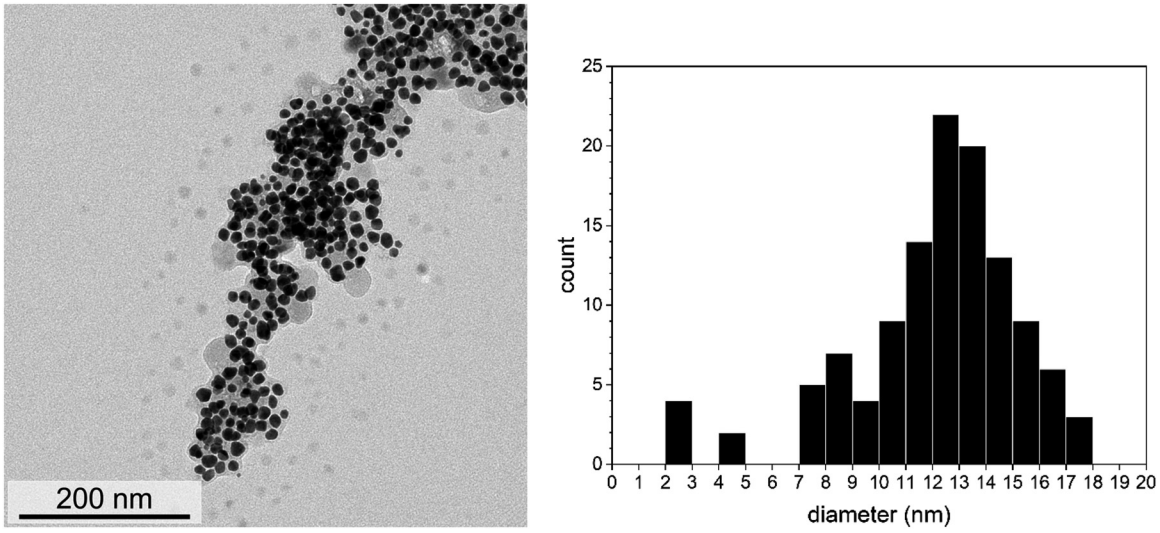

Figure 5: (Left) TEM image of mercury-free AuNPs [Method (B2)], and (right) the corresponding histogram of particle diameters. Several spherical AuNPs were visible with an average size of 12.2 ± 3.2 nm as assessed from 118 independent measurements.

The AuNPs labelled with radioactive mercury were stored for 2 months and subsequently measured by TEM., see Figure 7. The storage ensures that the Hg-197 has decayed, since the TEM did not accept radioactive samples. Several spherical AuNPs with a size of 12.3 ± 2.0 nm determined by measuring 489 different nanoparticles are visible. Again, the addition of radioactive Hg does not significantly change the shape or size of the nanoparticles. This result is consistent with our filtration and HPGe measurements.

All three batches of AuNPs (mercury-free, non-radioactive mercury spiked and $^{197m/g}$Hg labelled) were also measured by DLS methods, see Figure 8. The peaks of all three measurement are close to 20 nm, which corresponds with the results observed in the TEM images. This size difference between the TEM images and the DLS results is attributed to the hydrodynamic diameter that results from the particles suspended in solution, which creates a large diameter measured by DLS. The peaks at around 300 nm are most likely suspended aggregates or flocculates of AuNPs. The consistent size indicates the Hg had little effect on particle size, but the results also indicated that the AuNPs formed by incorporation of the radioactive Hg were relatively stable over a period of at least 2 months.

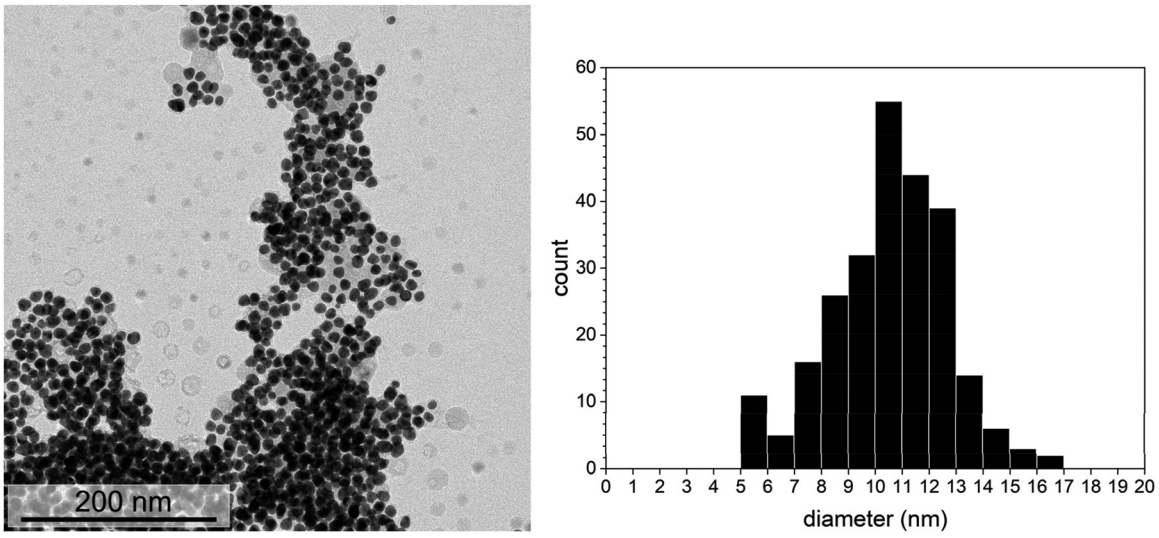

Figure 6: (Left) TEM image of mercury-spiked AuNPs [Method (B2)], and (right) the corresponding histogram of their diameters. Several spherical AuNPs were visible with an average size of 10.5 ± 2.2 nm as assessed from 253 independent measurements.

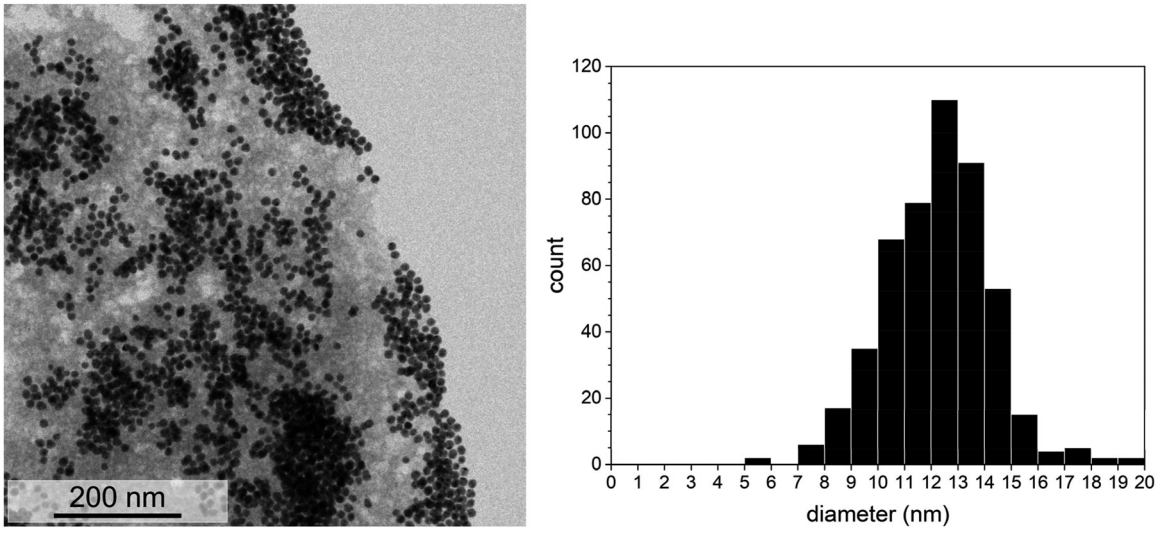

Figure 7: (Left) TEM image of mercury-labelled AuNPs [Method (B2)], and (right) the corresponding histogram of their diameters. Several spherical AuNPs were visible with an average size of 12.3 ± 2.0 nm as determined from 489 independent measurements.

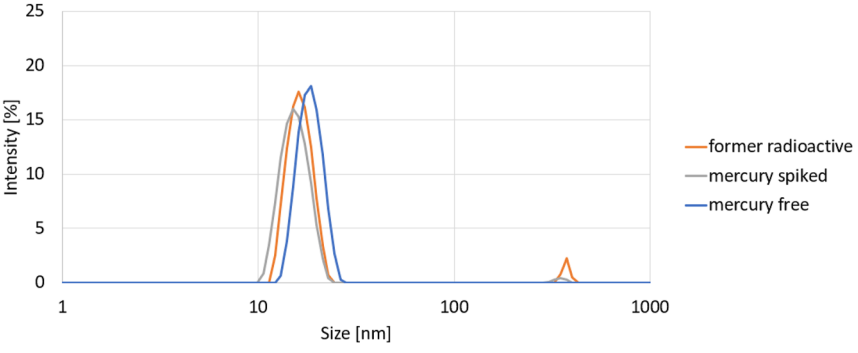

Figure 8: DLS spectra of the three different batches of AuNPs (i.e., without Hg, spiked with Hg, and Hg introduced via formation of radioactive AuNPs). The radioactive AuNPs were produced with Method (B2) and left to decay for two months before obtaining these measurements.

4 Conclusions

Our goal was to produce AuNPs that are labelled with $^{197m/g}$Hg and can be used in a medical application to treat glioblastomas. For this application, small gold nanoparticles with a narrow size-distribution were needed to reduce a large range of mobility in tissue. The results show that such AuNPs can be produced with tannic acid as a reducing agent. The resulting radioactive AuNPs had a size of 12.3 ± 2.0 nm according to results of TEM analyses and 15 ± 2 nm according to DLS measurements. The total activity of 151 ± 93 kBq (time corrected to EOB) was measured for the embedded Hg with a loading efficiency of 96 ± 7 % in the AuNPs with diameter smaller than 20 nm. This method has many advantages. First of all, it is fast, which is important when taking the half-life of $^{197m/g}$Hg into account (23.8 h for ^{197m}Hg and 64.14 h for ^{197g}Hg). The synthesis is also easy to perform as no complicated methods are needed. The AuNPs that are labelled with $^{197m/g}$Hg on their surfaces after their production have a risk of dislodging from the nanoparticles and releasing $^{197m/g}$Hg into solution. The nanoparticles in this project have demonstrated that the $^{197m/g}$Hg is likely embedded within the AuNPs and are not attached loosely to the surface of the AuNPs. Further work will evaluate the longer-term stability of the labelled AuNPs and will assess their performance for cytotoxicity *in vitro* and *in vivo*.

Acknowledgments: TRIUMF receives funding via a contribution agreement with the National Research Council of Canada (NRC). This research was funded by the National Sciences and Engineering Research Council of Canada (NSERC) via the Discovery grant program (RGPIN-2016-03972, RGPIN-2018-04997 & RGPIN-2020-06522). Additionally, this project was funded by a Canadian Cancer Society Innovation Grant (Award#: 706744). We would also like to thank the TR13 Cyclotron Operations Group consisting of Toni Epp, Ryley Morgan, Spencer Staiger, and led by David Prevost for regular irradiations of Au targets.

Author contributions: All the authors have accepted responsibility for the entire content of this submitted manuscript and approved submission.

Research funding: This work was supported by the NRC, NSERC (RGPIN-2016-03972, RGPIN-2018-04997 and RGPIN-2020-06522) and Canadian Cancer Society (706744).

Conflict of interest statement: The authors declare no conflicts of interest regarding this article.

References

1. Filosofov D., Kurakina E., Radchenko V. Potent candidates for targeted auger therapy: production and radiochemical considerations. *Nucl. Med. Biol.* 2021, *94*, 1.
2. Koning A. J., Rochman D., Sublet J. C., Dzysiuk N., Fleming M., van der Marck S. TENDL: complete nuclear data library for innovative nuclear science and technology. *Nucl. Data Sheets* 2019, *155*, 1.
3. Huang X., Zhou C. Nuclear data sheets for A = 197. *Nucl. Data Sheets* 2005, *104*, 283.
4. Ku A., Facca V. J., Cai Z., Reilly R. Auger electrons for cancer therapy–a review. *EJNMMI Radiopharm. Chem.* 2019, *4*, 1.
5. Parsons D. W., Jones S., Zhang X., Lin J. C. H., Leary R. J., Angenendt P., Mankoo P., Carter H., Siu I. M., Gallia G. L., Olivi A., McLendon R., Rasheed B. A., Keir S., Nikolskaya T., Nikolsky Y., Busam D. A., Tekleab H., Diaz L. A., Hartigan J., Smith D. R., Strausberg R. L., Marie S. K. N., Shinjo S. M. O., Yan H., Riggins G. J., Bigner D. D., Karchin R., Papadopoulos N., Parmigiani G., Vogelstein B., Velculescu V. E., Kinzler K. W. An integrated genomic analysis of human glioblastoma multiforme. *Science* 2008, *321*, 1807.
6. Lara-Velazquez M., Al-Kharboosh R., Jeanneret S., Vazquez-Ramos C., Mahato D., Tavanaiepour D., Rahmathulla G., Quinones-Hinojosa A. Advances in brain tumor surgery for glioblastoma in adults. *Brain Sci.* 2017, *7*, 166.
7. Oszvald A., Güresir E., Setzer M., Vatter H., Senft C., Seifert V., Franz K. Glioblastoma therapy in the elderly and the importance of the extent of resection regardless of age. *J. Neurosurg.* 2012, *116*, 357.
8. Georgiou C. J., Cai Z., Alsaden N., Cho H., Behboudi M., Winnik M. A., Rutka J. T., Reilly R. M. Treatment of orthotopic U251 human glioblastoma multiforme tumors in NRG mice by convection-enhanced delivery of gold nanoparticles labeled with the β-particle-emitting radionuclide, ^{177}Lu. *Mol. Pharm*. 2023, *20*, 582–592.
9. Haume K., Rosa S., Grellet S., Śmiałek M. A., Butterworth K. T., Solov'yov A. V., Prise K. M., Golding J., Mason N. J. Gold nanoparticles for cancer radiotherapy: a review. *Cancer Nanotechnol.* 2016, *7*, 1–20.
10. van Ballegooie C., Man A., Pallaoro A., Bally M., Gates B. D., Yapp D. T. Gold–protein composite nanoparticles for enhanced X-ray interactions: a potential formulation for triggered release. *Pharmaceutics* 2021, *13*, 1407.
11. Pekcevik I., Poon L., Wang M., Gates B. Tunable loading of single-stranded DNA on gold nanorods through the displacement of polyvinylpyrrolidone. *Anal. Chem.* 2013, *85*, 9960.
12. Piella J., Bastús N. G., Puntes V. Size-controlled synthesis of sub-10-nanometer citrate-stabilized gold nanoparticles and related optical properties. *Chem. Mater.* 2016, *28*, 1066.
13. Randhawa P., Olson A. P., Chen S., Gower-Fry K. L., Hoehr C., Engle J. W., Ramogida C. F., Radchenko V. Meitner-auger electron emitters for targeted radionuclide therapy: mercury-197m/g and antimony-119. *Curr. Rad.* 2021, *14*, 394.
14. Berger M. J., Coursey J. S., Zucker M. A., Chang J. Stopping-power & range tables for electrons, protons, and helium ions. *NIST Stand. Ref. Database* 2017, *124*, https://doi.org/10.18434/T4NC7P.
15. Prevost D., Jayamanna K., Graham L., Varah S., Hoehr C. New ion source filament for prolonged ion source operation on a medical cyclotron. *Instruments* 2019, *3*, 5.
16. Daumann S. *Synthese und Charakterisierung von Nanopartikeln: Anisotrope Edelmetall-Nanopartikel und Zinkoxid-Nanopartikel*; Universitätsbibliothek Duisburg-Essen: Duisburg-Essen, 2017.
17. Turkevich J., Stevenson P. C., Hillier J. A study of the nucleation and growth processes in the synthesis of colloidal gold. *Discuss. Faraday Soc.* 1951, *11*, 55.
18. Hatschek E. Laboratory manual of elementary colloid chemistry. *Nature* 1926, *117*, 447.